E-Article

Slowing Down in Spatially Patterned Ecosystems at the Brink of Collapse

Vasilis Dakos,[1,*] Sonia Kéfi,[2] Max Rietkerk,[3] Egbert H. van Nes,[1] and Marten Scheffer[1]

1. Department of Aquatic Ecology and Water Quality Management, Wageningen University, P.O. Box 47, 6700AA Wageningen, The Netherlands; 2. J. F. Blumenbach Institute of Zoology and Anthropology, Georg-August-Universität Göttingen, Berliner Str. 28, 37073 Göttingen, Germany; and Université Montpellier 2, Centre National de la Recherche Scientifique, Institut des Sciences de l'Evolution, 34095 Montpellier, Cedex 05, France; 3. Department of Environmental Sciences, Utrecht University, P.O. Box 80115, 3508 TC Utrecht, The Netherlands

Submitted July 26, 2010; Accepted January 25, 2011; Electronically published April 26, 2011

abstract: Predicting the risk of critical transitions, such as the collapse of a population, is important in order to direct management efforts. In any system that is close to a critical transition, recovery upon small perturbations becomes slow, a phenomenon known as critical slowing down. It has been suggested that such slowing down may be detected indirectly through an increase in spatial and temporal correlation and variance. Here, we tested this idea in arid ecosystems, where vegetation may collapse to desert as a result of increasing water limitation. We used three models that describe desertification but differ in the spatial vegetation patterns they produce. In all models, recovery rate upon perturbation decreased before vegetation collapsed. However, in one of the models, slowing down failed to translate into rising variance and correlation. This is caused by the regular self-organized vegetation patterns produced by this model. This finding implies an important limitation of variance and correlation as indicators of critical transitions. However, changes in such self-organized patterns themselves are a reliable indicator of an upcoming transition. Our results illustrate that while critical slowing down may be a universal phenomenon at critical transitions, its detection through indirect indicators may have limitations in particular systems.

Keywords: leading indicators, resilience, alternative stable states, early warning signals, local facilitation, scale-dependent feedback.

Introduction

There is growing evidence that some ecosystems may occasionally undergo catastrophic transitions to alternative states (Scheffer et al. 2001). Coral reefs can be overgrown by fleshy algae and shift to a degraded state (Knowlton 1992), shallow lakes may flip from a macrophyte-dominated clear water state to a turbid water state as a result of eutrophication (Scheffer 1998), and arid ecosystems may lose their perennial vegetation and turn into desert as a result of increasing aridity or overgrazing (Millennium Assessment 2005; Reynolds et al. 2007).

Close to a critical threshold for such catastrophic transitions, the resilience (sensu Holling 1973) of an ecosystem becomes small in the sense that only a small perturbation is needed to tip the ecosystem to an alternative state. Intuitively, such a loss of resilience can be understood as the shrinking of the basin of attraction around the equilibrium state of the ecosystem (fig. 1). Unfortunately, our knowledge of most ecosystems or other systems is insufficient to predict critical thresholds, while at the same time it is difficult to measure resilience directly (Carpenter 2003). In view of these limitations, an alternative approach has been recently proposed (Scheffer et al. 2009).

The idea is to use generic properties of critical thresholds (bifurcation points) to develop early warning indicators that can be used as indirect indicators of resilience (Scheffer et al. 2009). These indicators are simple statistical properties that can be measured directly by monitoring the state variables of the system, and they all behave in predictable ways before transitions, regardless of the details of the system. In other words, theory suggests that we can identify the risk of an upcoming transition by monitoring characteristics such as population abundances, nutrient concentrations, or vegetation cover in any system, be it a coral reef, a lake, or a savanna ecosystem.

The fact that these indicators change predictably before critical transitions is related to the return rate to equilibrium after a perturbation that goes to zero at most bifurcations. To see what this means intuitively, note that when the basin of attraction shrinks, it also becomes flatter (fig. 1). This implies that the monitored state variable of the system—such as macrophyte cover in a lake—returns more slowly to equilibrium after a small perturbation (fig. 1*B*; Wissel 1984). This phenomenon, known as critical

* Corresponding author; e-mail: vasileios.dakos@wur.nl.

Am. Nat. 2011. Vol. 177, pp. E153–E166.
DOI: 10.1086/659945

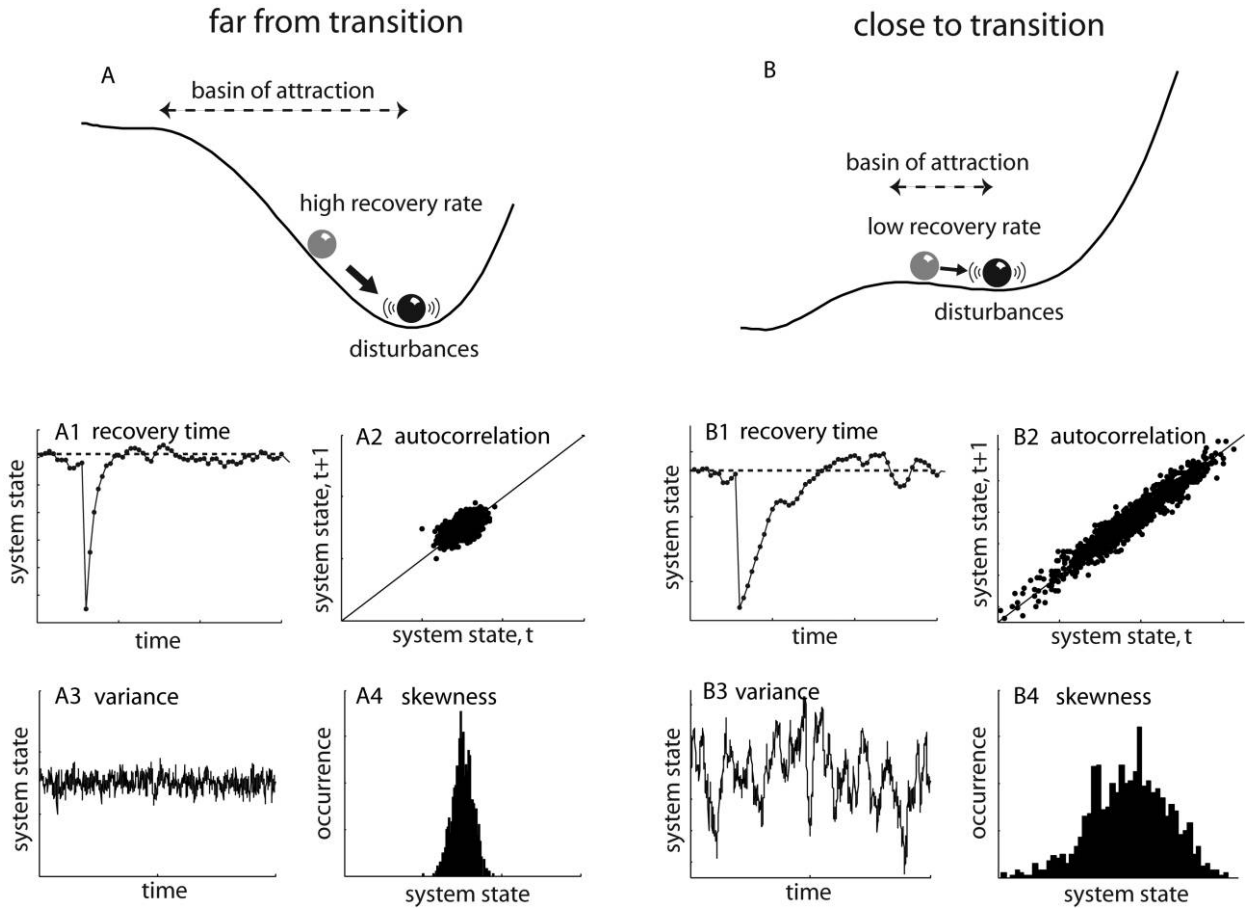

Figure 1: Balls and cups representation of the basin of attraction of a system with alternative stable states. *A*, Far from transition, the state of the system lies in a broad basin of attraction. Small disturbances to equilibrium are damped by high recovery rates back to equilibrium. As a result, the time to recover from a disturbance is short (*A1*). When monitoring the state of the system in time, the time series is characterized by low correlation between subsequent values (*A2*), low variance (*A3*), and low skewness (*A4*). *B*, Close to transition, the basin of attraction shrinks and may become asymmetric. Small disturbances increase the chance of shifting to the alternative state, and they are no longer effectively damped as a result of low recovery rates back to equilibrium. The time to recover from a disturbance now is long (critical slowing down; *B1*), and the collective time series is characterized by high correlation between subsequent values (*B2*), high variance (*B3*), and high skewness (*B4*).

slowing down (Strogatz 1994), has major consequences for the transient behavior of the system. A system will take longer to recover from a disturbance when it is close to a critical threshold (van Nes and Scheffer 2007; fig. 1, *A1*, *B1*). If the system is subjected to stochastic perturbations, there are also systematic changes in its fluctuations. First, it will resemble its previous state more closely when it is close to a critical threshold (Ives et al. 2003; Held and Kleinen 2004; fig. 1, *A2*, *B2*). Second, the state of the system will fluctuate more widely around its equilibrium close to transition (van Nes and Scheffer 2003; Carpenter and Brock 2006; fig. 1, *A3*, *B3*). Usually, but not necessarily, the basin of attraction also becomes asymmetric close to a transition (fig. 1; Scheffer et al. 2009). Such asymmetry causes the state of the system to spend more time in the flatter part of the attraction basin (fig. 1, *A4*, *B4*). As a result, the distribution of system states becomes skewed near a transition (Guttal and Jayaprakash 2008). While most of the work on leading indicators has focused on the analysis of time series, the temporal indicators that signal approaching shifts have spatial equivalents as well. This means that we can also measure leading indicators using spatial information for systems such as the distribution of abundances of metapopulations in a fragmented habitat or the distribution of vegetation over a landscape. In such cases, spatial correlation may rise (Dakos et al. 2010), spatial variance may increase (Guttal and Jayaprakash 2009; Donangelo et al. 2010), and spatial skewness will often

peak (Guttal and Jayaprakash 2009) before a spatially connected system goes through a systemic shift to an alternative state.

So far, most of these indicators have been tested in relatively simple models where a specific type of critical transition occurs (i.e., a fold or transcritical bifurcation; Carpenter and Brock 2006; van Nes and Scheffer 2007; Guttal and Jayaprakash 2008). In such simple models, the indicators work well. There are, however, other cases of critical transitions for which it is not yet clear whether these indicators would successfully work (Scheffer et al. 2009; Hastings and Wysham 2010). Spatially explicit ecosystems with pattern formation are such a case (Rietkerk et al. 2004).

Pronounced examples of such patterned ecosystems come from arid ecosystems where we can find a mosaic of vegetated patches and bare soil (Aguiar and Sala 1999). Climate change and human pressure may cause these systems to turn into barren deserts (Reynolds et al. 2007), with considerable consequences for the livelihoods of more than 25% of the world's population. Specific models have shown that the collapse of vegetation to bare soil can be a critical transition (Rietkerk et al. 2002). Depending on the spatial mechanisms that dominate in arid ecosystems, particular changes in spatial patterns may signal whether vegetation is close to collapsing into bare ground. A class of models stressing local facilitation predicts changes in the size distribution of vegetation patches before desertification (Kéfi et al. 2007*b*, 2011). Another class of models stresses that when resources accumulate in the vicinity of vegetation but are depleted elsewhere (Rietkerk et al. 2002), regular self-organized patterns occur. In these models, pattern shapes are predicted to change in specific ways before the collapse to a desert state (von Hardenberg et al. 2001; Rietkerk et al. 2004). Remarkably, the universal phenomenon of critical slowing down—and the way this may translate into the generic leading indicators of correlation and variance—has not been studied in such spatially patterned systems so far. Obviously, combining generic and specific leading indicators in this type of spatial systems can advance our ability to anticipate critical transitions.

Here, we address this gap in our understanding of the predictability of critical transitions in spatially patterned models, using arid ecosystems as an example. First, we explore whether critical slowing down occurs before the collapse to desertification in these models. We then estimate both spatial and temporal early warning indicators and compare them with the specific pattern-based indicators found in these systems when approaching a critical transition.

Methods

Three Models of Desertification: Spatial Mechanisms, Patterns, and Transitions

We analyzed three existing models that describe spatial dynamics of vegetation in arid ecosystems. All models may undergo a critical transition to a desert state, but they differ in the type of patterns they exhibit. All transitions are associated with hysteresis. This means that restoring environmental conditions to values before the transition does not lead to recovery of vegetation. Here we describe the mechanisms, transitions, and patterns encountered in each model.

The first model is based on the vegetation model by Shnerb et al. (2003) and Guttal and Jayaprakash (2007):

$$\frac{dw_{i,j}}{dt} = R - w_{i,j} - \lambda w_{i,j} B_{i,j} \tag{1a}$$

$$+ D(w_{i+1,j} + w_{i-1,j} + w_{i,j+1} + w_{i,j-1} - 4w_{i,j}) + \sigma_w dW_{i,j},$$

$$\frac{dB_{i,j}}{dt} = \rho B_{i,j}\left(w_{i,j} - \frac{B_{i,j}}{B_c}\right) - \mu \frac{B_{i,j}}{B_{i,j} + B_O} \tag{1b}$$

$$+ D(B_{i+1,j} + B_{i-1,j} + B_{i,j+1} + B_{i,j-1} - 4B_{i,j}) + \sigma_B dW_{i,j}.$$

We made this model spatially explicit by defining it as a stochastic lattice differential equation model (Chow et al. 1996). In such a model, space is represented by a two-dimensional lattice of coupled patches (Keitt et al. 2001; van Nes and Scheffer 2005). In each patch, vegetation B grows logistically and has a loss rate due to grazing. Vegetation growth depends on water availability w. When annual rainfall decreases, water scarcity reduces vegetation growth. At some point, vegetation growth cannot compensate for losses to grazing, and a patch shifts to its alternative overgrazed desert state. Biomass and water are exchanged between neighboring patches at rate D. Therefore, a patch with high biomass will have the tendency to "leak" biomass to its neighboring sites, which results in a positive effect on its neighbors (in terms of biomass gain) but a negative effect on the site itself (fig. 2, *A1*). If this diffusive effect is very strong, differences between patches tend to be smoothed out, and the ecosystem as a whole remains in a homogeneously vegetated state (fig. 2, *A2*), until conditions force all patches to flip to the desert state through synchronized "fold bifurcations" at each patch (fig. 2, *A3*; van Nes and Scheffer 2005). (Bifurcations occur at parameter values where the qualitative behavior of a system changes fundamentally.) The important mechanism in this model is a positive feedback that causes each patch to have alternative stable states (undergrazed vegetated state or overgrazed desert state). For this reason, we refer to this model as the local positive feedback model.

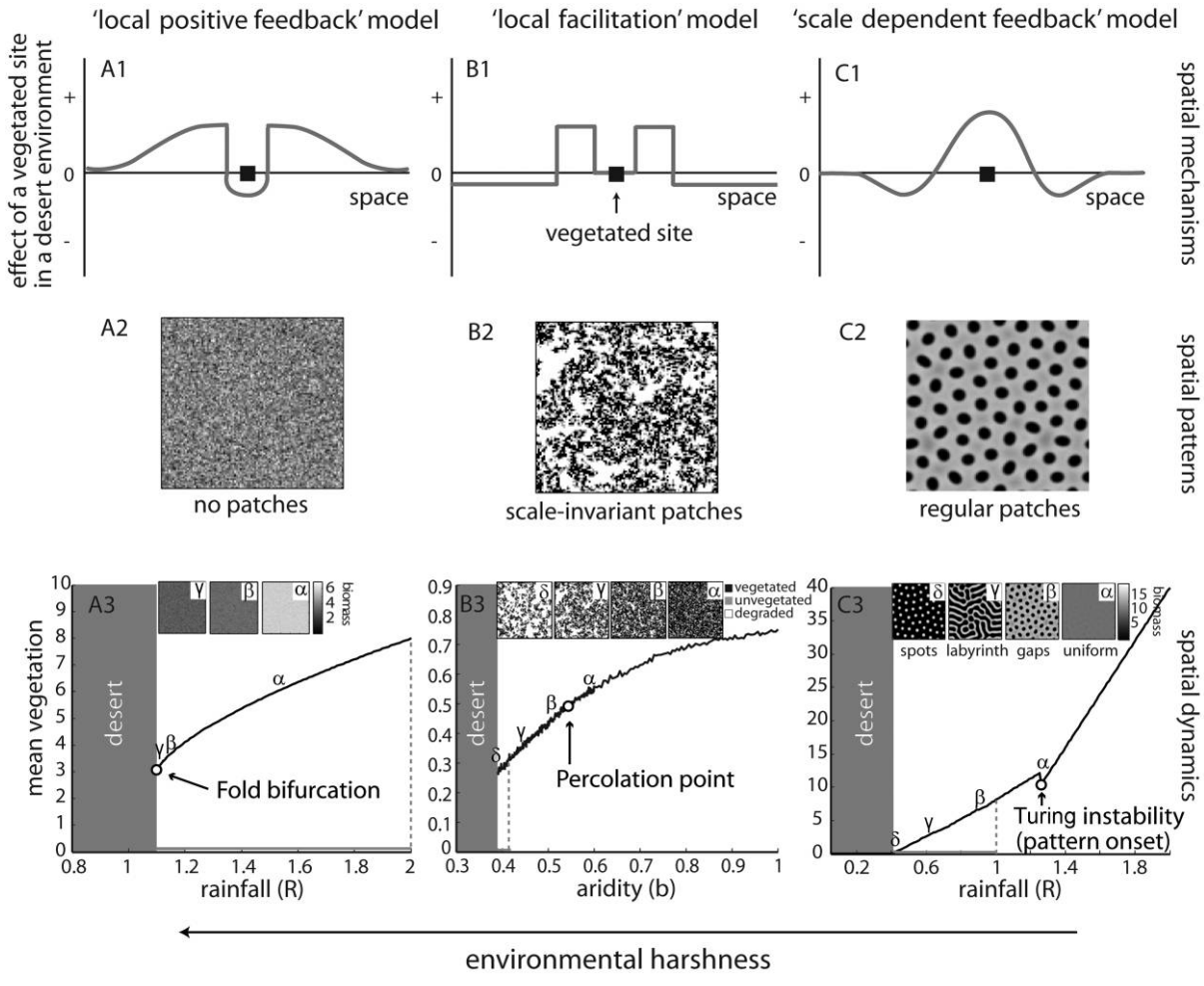

Figure 2: Schematic representation of the effect of vegetation on its environment, the patterns formed, and the dynamics of vegetation as a function of environmental harshness. *A*, Local positive feedback model. *A1*, A vegetated site with high vegetation biomass has a positive effect on its environment but a negative effect on itself because of a "leak" of biomass to neighboring sites. The positive effect diminishes with distance. *A2*, No patches form, only irregular clustering of biomass. *A3*, Spatial vegetation mean biomass with decreasing rainfall *R*. *B*, Local facilitation model. *B1*, A vegetated site has a positive effect in its direct vicinity, with no cost to itself. *B2*, Irregular vegetation patches form. *B3*, Spatial vegetation density (fraction of vegetation sites occupied) with decreasing aridity *b*. *C*, Scale-dependent feedback model. *C1*, A vegetated site has a positive impact on itself and its surroundings but negative feedback farther away because local accumulation of water means that water is depleted farther away. *C2*, Regular vegetation patterns form. *C3*, Spatial vegetation mean density with decreasing rainfall *R*. Regardless of the spatial mechanisms in each model, there is a critical point at which vegetation collapses (*shaded area*). Fold bifurcation: point at which total vegetation shifts to desert; percolation point: breakup of giant cluster that spans the whole lattice; Turing instability: onset of regular pattern formation. Insets are spatial snapshots of vegetation before desertification. Dotted gray lines indicate the hysteresis loop present in all systems.

The second model is a stochastic cellular automaton (Kéfi et al. 2007*a*) with discrete time steps:

$$w_{\{0,+\}} = [\delta\rho_+ + (1-\delta)q_{+|0}](b - c\rho_+), \quad (2a)$$

$$w_{\{-,0\}} = r + fq_{+|-}, \quad (2b)$$

$$w_{\{+,0\}} = m, \quad (2c)$$

$$w_{\{0,-\}} = d. \quad (2d)$$

An ecosystem is represented by a lattice composed of cells, which can be in one of three states: vegetated (+), empty (0), or degraded (−). Empty cells are cells whose soil is still fertile. Degraded cells are cells with eroded soil unsuitable for recolonization. The basic processes in this model are captured by four transformations: colonization of empty cells, mortality of vegetation, degradation of empty cells, and regeneration of degraded cells. Each of these four transformations can occur with a certain prob-

ability at each time step (eqq. [2]). The colonization and regeneration probabilities of a patch are positively affected by the presence of vegetation in its four neighboring cells (fig. 2, *B1*). Because of this facilitating effect, we will refer to this model hereafter as the local facilitation model. The facilitation leads to the formation of clusters of vegetated grid cells, and these patches have size distributions that can be described by a power law (fig. 2, *B2*; Kéfi et al. 2007*b*, 2011). The size of the clusters is dependent on the ecological conditions (such as rainfall or grazing pressure). Under favorable conditions, giant clusters span the lattice from one edge to the other (Kéfi et al. 2011). The point where these giant clusters break down is called the percolation point. When conditions become even harsher, a transition point is reached where all vegetation becomes extinct (fig. 2, *B3*).

The third model is a stochastic version of a partial differential equations model describing the dynamics of vegetation biomass, soil water, and surface water (HilleRisLambers et al. 2001; Rietkerk et al. 2002):

$$\frac{\partial P}{\partial t} = cg_{\max}\frac{W}{W + k_1}P - dP + D_P\Delta P + \sigma dW, \quad (3a)$$

$$\frac{\partial W}{\partial t} = \alpha O\frac{P + k_2W_O}{P + k_2} - cg_{\max}\frac{W}{W + k_1}P - r_WW + D_W\Delta W + \sigma dW, \quad (3b)$$

$$\frac{\partial O}{\partial t} = R - \alpha O\frac{P + k_2W_O}{P + k_2} + D_O\Delta O + \sigma dW. \quad (3c)$$

Plants (P) grow depending on soil water availability and are lost as a result of mortality or grazing. Surface water (O) is supplied by rainfall and lost due to infiltration in the soil and runoff. Soil water (W) is surface water that infiltrates the soil after rain events and is taken up by plants or lost by runoff. Plants, soil water, and surface water are all assumed to diffuse in two-dimensional space. In this model, the infiltration rate of water in the soil is higher in areas with vegetation than in bare soil, leading to accumulation of water under vegetation and to its depletion farther away, a scale-dependent feedback. In other words, vegetation has a local positive effect on itself and on its immediate surroundings but a negative effect farther away (fig. 2, *C1*). For this reason, we refer to this model as the scale-dependent feedback model. This scale-dependent feedback leads to the formation of regular vegetation patterns (fig. 2, *C2*, *C3*) through a so-called Turing instability (Turing 1952). At the Turing instability, the feedback is just strong enough to form patterns (HilleRisLambers et al. 2001; von Hardenberg et al. 2001; Rietkerk et al. 2002). Patterns show a distinct sequence of shapes, from gaps to labyrinths to spots with decreasing rainfall. When water availability becomes limited, vegetation cannot sustain itself, and the ecosystem undergoes a second transition point: that of collapse into desert (fig. 2, *C3*).

Simulations and Analyses

Parameter values of the three models and their units are given in table 1. We used parameter values such that the transition of vegetation to desertification is discontinuous (catastrophic). In all models, we assumed homogeneous conditions; that is, parameter values are the same everywhere in space. For each model, we selected a parameter that describes aridity (see table 1), since this drives desertification in arid ecosystems. In the local positive feedback and scale-dependent feedback models, the level of aridity is directly determined by rainfall (parameter R; low rainfall leads to low vegetation growth), whereas in the local facilitation model, aridity is indirectly determined by the establishment probability of new vegetation (parameter b; high aridity leads to low vegetation establishment). In all models, we changed these control parameters in small steps. We started simulations from a complete vegetated state in all models. We discarded transients and continued the simulations in each step, using the last stationary state as the initial condition. We repeated this until the control parameters reached a critical threshold at which vegetation collapsed.

We first examined whether critical slowing down occurs before all transition points in all models. Because there are no formal analytical solutions for all transitions that could enable us to estimate critical slowing down by the dominant eigenvalue of the system (Scheffer et al. 2009), we followed a numerical approach (van Nes and Scheffer 2007). After the ecosystem reached equilibrium, we removed 10% of the total vegetation biomass, cover, or density according to model and estimated the recovery time to equilibrium (with an accuracy of 0.01%) by simulation. We did this along the whole pathway to collapse of vegetation for all models.

For the calculation of the spatial indicators, we used equilibrium values of vegetation biomass, cover, or density according to the model for each level of control parameter up to collapse of vegetation. In the case of the local facilitation model, we first determined the vegetation cover by summing the vegetated cells using a 4 × 4-cell nonoverlapping moving filter along the lattice. We estimated spatial correlation between neighbors, spatial variance, and spatial skewness. Spatial correlation between neighbors was defined as the two-point correlation for all pairs of neighboring cells using Moran's coefficient (Legendre and Fortin 1989). Skewness was estimated as the third moment about the mean, $[\mathrm{E}(x - \mu)^3]/\sigma^3$, where μ is the mean of

Table 1: Model parameters and their values

Model parameter	Definition	Value and unit
Local positive feedback model:[a]		
$w_{i,j}$	Water moisture level in each grid cell (i, j)	mm
$B_{i,j}$	Vegetation biomass in each grid cell (i, j)	g
D	Exchange rate	.05 day^{-1}
λ	Water consumption rate by vegetation	.12 g^{-1} day^{-1}
ρ	Maximum vegetation growth rate	day^{-1}
B_c	Vegetation carrying capacity	1 g
μ	Maximum grazing rate	2 day^{-1}
B_O	Half-saturation constant of vegetation consumption	1
R	Mean annual rainfall[b]	.8–2 mm day^{-1}
σ_W	Standard deviation of white noise on water moisture	.01
σ_B	Standard deviation of white noise on vegetation biomass	.25
$dW_{i,j}$	White noise; uncorrelated in each grid cell (i, j)	
Local facilitation model:[c]		
$w_{\{0,+\}}$	Colonization probability of an unoccupied site	
$w_{\{-,0\}}$	Regeneration probability of a degraded site	
$w_{\{+,0\}}$	Mortality probability of an occupied site	
$w_{\{0,-\}}$	Degradation probability of an unoccupied site	
ρ_+	Density of vegetated sites	
$q_{i\|j}$	Clustering vegetation intensity probability of finding a site j in state i $(+, 0, -)$	
m	Mortality probability of a vegetated site	.1
f	Local facilitation strength: maximum effect of a neighboring vegetated site on the regeneration of a degraded site	.9
β	Intrinsic seed production rate per vegetated site; "survival probability," "germination probability"	
ε	Establishment probability of seeds on {0} site in a system without competition	
b	Measures the severity of the environmental conditions $(=\beta\varepsilon)$; a lower b value reflects a higher aridity level[b]	.3–1
δ	Fraction of seeds globally dispersed	.1
g	Competitive effect of the global density of {+} sites on the establishment of new individuals	
c	βg	.3
r	Regeneration probability of a {−} site without vegetated sites in its neighborhood	.0001
d	Degradation probability of {0} sites	.2
Scale-dependent feedback model:[d]		
P	Plant density	g m^{-2}
W	Soil water	mm
O	Surface water	mm
c	Conversion of water uptake to plant growth	10 g mm^{-1} m^{-2}
g_{max}	Maximum specific water uptake	.05 mm g^{-1} m^{-2} day^{-1}
k_1	Half-saturation constant of specific plant growth and water uptake	5 mm
D_p	Plant dispersal	.1 m^{-2} day^{-1}
α	Maximum infiltration rate	.2 day^{-1}
k_2	Saturation constant of water infiltration	5 g m^{-2}
W_O	Water infiltration rate in the absence of plants	.2
r_W	Specific water loss due to evaporation and drainage	.2 day^{-1}
D_W	Diffusion coefficient of soil water	.1 m^2 day^{-1}
D_O	Diffusion coefficient of surface water	100 m^2 day^{-1}
d	Specific loss of plant density due to mortality	.25 day^{-1}
Δ	Laplacian operator for diffusion	
R	Rainfall[b]	.05–2 mm day^{-1}
σ	Standard deviation of white noise	.01
dW	White noise	

[a] Equations (1); modified from Guttal and Jayaprakash (2007).

[b] Control parameter that determines the collapse of vegetation at a critical value.

[c] Equations (2); from Kéfi et al. (2007*a*).

[d] Equations (3); modified from Rietkerk et al. (2002).

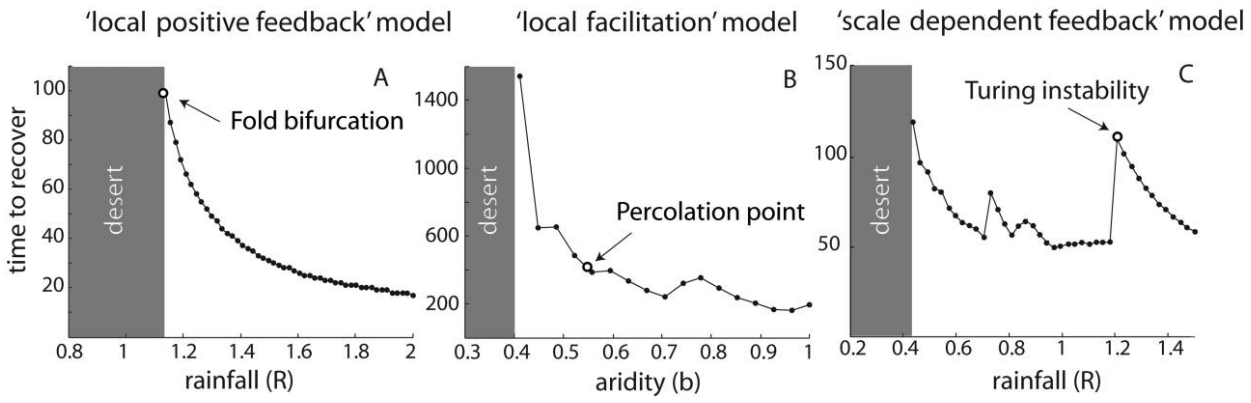

Figure 3: Critical slowing down approximated by recovery time before the collapse of vegetation in all three models. Recovery time was estimated by a pulse perturbation experiment as the time for mean plant density to recover back to equilibrium after a 10% reduction in plant densities in the whole lattice. Results based on simulations in a 64 × 64-cell lattice for the local positive feedback and scale-dependent feedback models. All other parameters are as presented in the text.

x, σ is the standard deviation of x, and E(.) is the expectation operator.

In addition to spatial indicators, we also followed the evolution of temporal correlation, variance, and skewness. To this end, for each level of control parameter, we estimated autocorrelation at lag 1, variance, and skewness of total vegetation biomass, cover, or density from the last 1,000 points of the produced time series. We calculated autocorrelation at lag 1 by fitting an autoregressive model of first order using the arfit package in MATLAB (Neumaier and Schneider 2001). To compare the performance of both spatial and temporal indicators, we quantified their trends using the nonparametric Kendall τ rank correlation of the control parameter and the spatial and temporal correlation estimates. A Kendall τ coefficient that was significantly different from 0 ($P < .025$) specified whether the indicators increased or decreased before each transition point.

All simulations and statistical analyses were performed in MATLAB (ver. 7.1.0246; Mathworks). We solved the stochastic equations of the local positive feedback model in a 100 × 100-cell lattice using an Euler-Murayama integration method with Ito calculus. We used a stochastic asynchronous update algorithm for the local facilitation model in a 400 × 400-cell lattice. The scale-dependent feedback model was implemented in a 128 × 128-cell lattice and solved using a semi-implicit method (Janssen et al. 2008). The stochastic part of the scale-dependent feedback model was solved using an Euler-Murayama integration method with Ito calculus. We assumed periodic boundaries in all models.

Results

Critical Slowing Down before Transitions

We first checked whether critical slowing down was present before each transition point in all models. In all models, we found an increase in time needed for recovery as the ecosystem approached the critical point of collapse to a desert state (fig. 3). Similarly, recovery times increased before the Turing instability point in the scale-dependent feedback model (fig. 3*C*). All these points belong to the type of transitions where critical slowing down is expected to occur; they represent local bifurcations of stable equilibria that become unstable (Judd and Silber 2000; Kéfi et al. 2007*b*; Dakos et al. 2010). Interestingly, critical slowing down also occurred before the vegetation collapse in the scale-dependent feedback model, despite the fact that this transition represents a more complicated kind of bifurcation. Specifically, it corresponds to a global bifurcation, where a stable spatial periodic attractor (the regular vegetation patterns) collapses to a uniform desert state. Obviously, the percolation point in the local facilitation model cannot be detected by critical slowing down, since this point does not correspond to a bifurcation that would imply a change in the stability of the ecosystem.

Spatial Leading Indicators before Transitions

For the transitions where critical slowing down was at play, we tested whether spatial correlation, variance, and skewness also increased (see table A1). In the local positive feedback model, all of these spatial indicators showed clear

positive trends before the transition (fig. 4, *A1–A3*), similar to those observed in previous studies (Guttal and Jayaprakash 2009; Dakos et al. 2010). Close to collapse, slowly decaying fluctuations of vegetation resulted in an increase in spatial variance. Because these fluctuations took place in an increasingly asymmetric basin of attraction, spatial skewness changed as well (it became negative because vegetation biomass distributions skewed toward low biomass values).

In the local facilitation model, the three spatial indicators behaved more or less the same as in the local positive feedback model (fig. 4, *B1–B3*). Far from the transition, environmental conditions sustained large areas of vegetation cover, leading to low spatial variance (fig. 4, *B1*). Spatial skewness was negative, since distributions of vegetation cover were skewed toward low values (fig. 4, *B2*). As aridity increased, areas of high vegetation cover broke into smaller parts; vegetation cover distributions became symmetric, and therefore variance increased and skewness became zero. Approaching the transition, skewness turned positive, because now areas of high vegetation cover became scarce. Variance of vegetation cover also rose toward the transition, only to drop just before the shift. Spatial correlation between neighbors gradually increased up to the transition (fig. 4, *B3*). As expected, no special change occurred before the percolation point. In addition to spatial correlation, variance, and skewness, changes in patch size distributions also indicated proximity to desertification (fig. 5*A*).

In the scale-dependent feedback model, the onset of

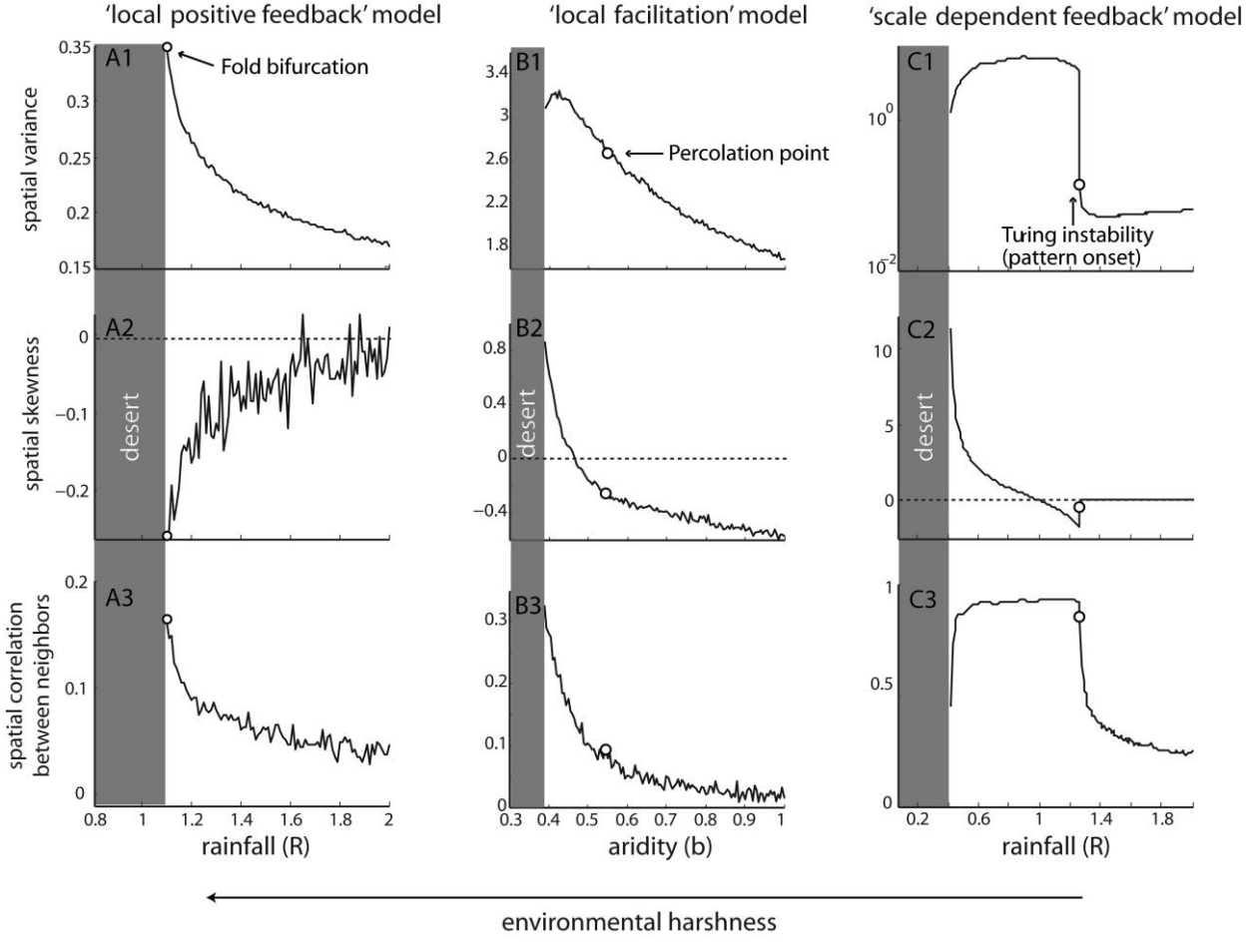

Figure 4: Spatial variance, spatial skewness, and spatial correlation between neighbors as a function of increasing harshness in the environment up to desertification (*shaded area*). Spatial indicators are estimated using final values of all cells at the end of the simulation for each level of the control parameter (rainfall in local positive feedback and scale-dependent feedback models; aridity in local facilitation model). Open circles indicate the point at which vegetation shifts to a barren state in the local positive feedback model (fold bifurcation; *A1–A3*), the point at which patches of vegetation that span the lattice from one edge to the other disappear in the local facilitation model (percolation point; *B1–B3*), and the onset of regular vegetation patterning in the scale-dependent feedback model (Turing instability; *C1–C3*).

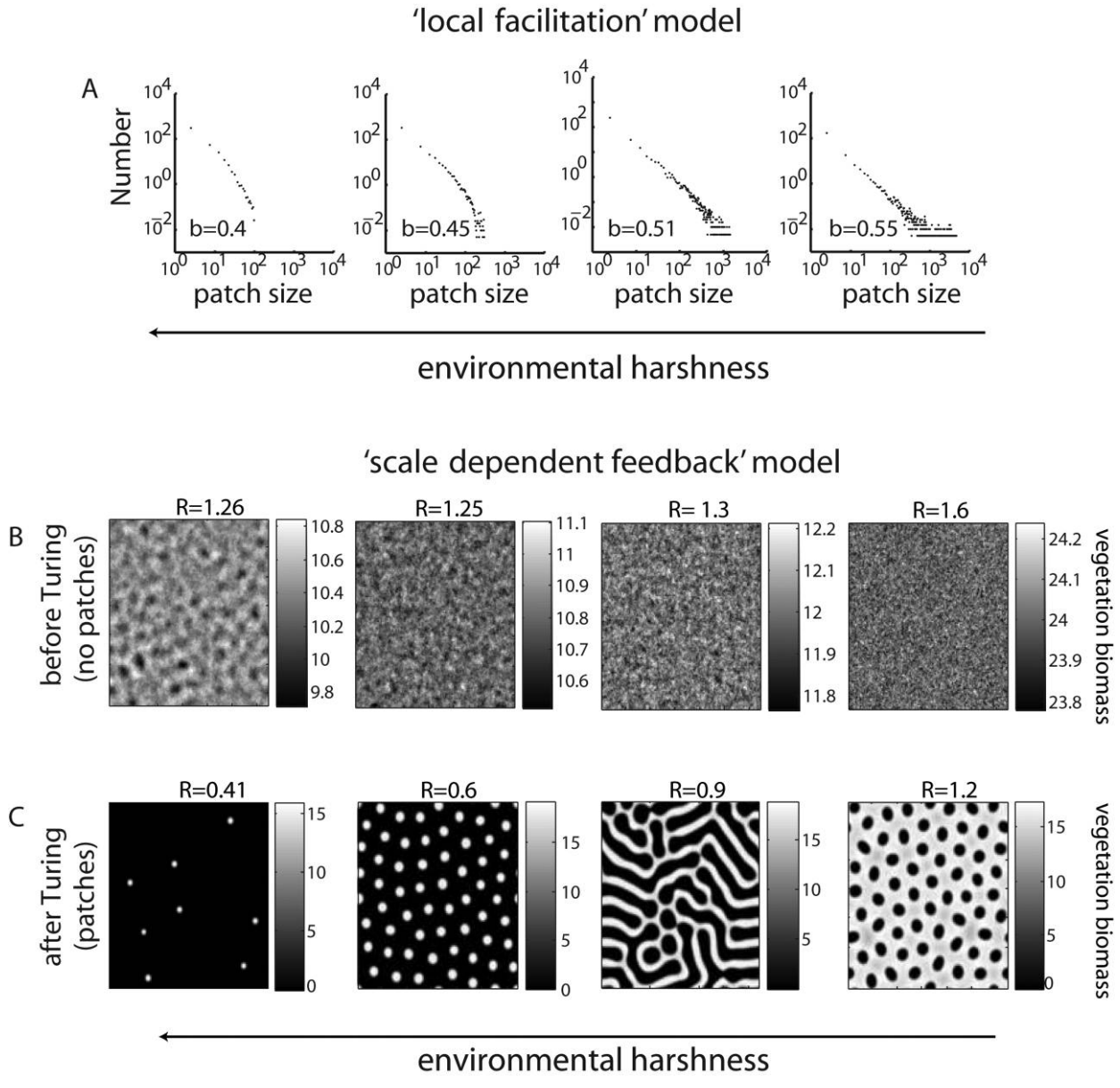

Figure 5: System-specific indicators. *A*, Local facilitation model: evolution of patch size distributions. As conditions become harsher, big vegetated patches disappear, and their distribution is characterized by a truncated power law. Statistical properties of the changing distributions are summarized in figure A1. *B*, Scale-dependent feedback model: spatial configuration of vegetation before the Turing instability for decreasing rainfall (R). Note the slight emergence of patterns before the Turing instability ($R \approx 1.25$; scale in all panels is comparable). *C*, After the Turing instability, there is a specific sequence of pattern shapes: gaps, labyrinth, spots, and the gradual loss of spots until the system collapses.

pattern formation at the Turing instability point was again announced by an increase in spatial correlation between neighbors and variance (fig. 4, *C1–C3*), as would be expected in view of the critical slowing down we found (fig. 3*C*). Spatial skewness remained constant (fig. 4, *C2*), since there is no alternative attractor (bare ground) before the onset of pattern formation. Despite the presence of critical slowing down, spatial correlation or variance did not increase before the collapse of vegetation in the scale-dependent feedback model (fig. 4, *C1–C3*). There was an increase in spatial skewness. However, this was driven by the increasing number of bare cells in the lattice due to

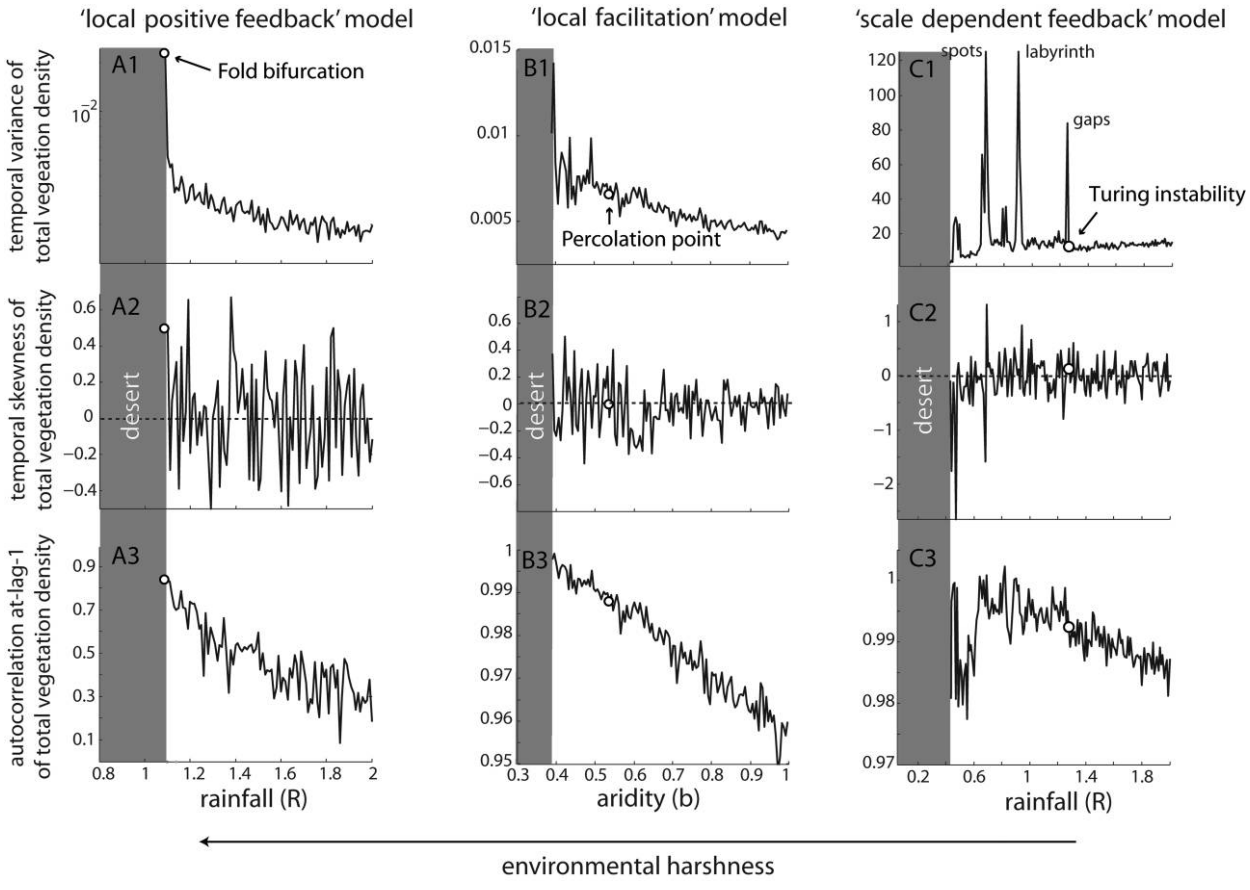

Figure 6: Temporal variance, temporal skewness, and temporal autocorrelation (at lag 1) as functions of increasing harshness in the environment up to desertification (*shaded area*). Temporal indicators are estimated from the last 1,000 points of total vegetation biomass, cover, or density for each level of control parameter (rainfall in local positive feedback and scale-dependent feedback models; aridity in local facilitation model). Open circles indicate the point at which vegetation shifts to a barren state in the local positive feedback model (fold bifurcation; *A1–A3*), the point at which patches of vegetation that span the lattice from one edge to the other disappear in the local facilitation model (percolation point; *B1–B3*), and the onset of regular vegetation patterns in the scale-dependent feedback model (Turing instability; *C1–C3*).

the gradual loss of vegetation rather than to an asymmetric basin of attraction. Spatial variance stayed high as patterns evolved from gaps to labyrinths but decreased when spots emerged and dropped just before the ecosystem turned into desert (fig. 4, *C1*). Spatial correlation of vegetation density was high and dropped only shortly before the collapse, when the regularity in the shape of the patterns became weaker (fig. 4, *C3*). While spatial correlation and variance did not change as the ecosystem approached this transition, the sequence in the shape of vegetation patterns clearly indicated the upcoming collapse (fig. 5*C*).

Temporal Leading Indicators before Transitions

In addition to spatial correlation, variance, and skewness, we estimated temporal autocorrelation (at lag 1), variance, and skewness for the total vegetation cover in all models (fig. 6). In the local positive feedback and local facilitation models, autocorrelation (at lag 1) and variance increased toward the transition (fig. 6, *A1*, *A3*, *B1*, *B3*). Temporal skewness did not change in any of the two models (fig. 6, *A2*, *B2*). In the scale-dependent feedback model, all temporal indicators failed to signal upcoming desertification (fig. 6, *C1–C3*). Peaks in variance of total vegetation density after the Turing instability occurred almost when patterns changed from gaps to labyrinths to spots (fig. 6, *A1*). Similarly but less clearly, peaks in skewness after the Turing instability were related to transitions in the sequence of patterns (fig. 6, *C2*). Autocorrelation (at lag 1) after the Turing instability remained high and fluctuated slightly as more cells became bare before the transition (fig. 6, *C3*). Interestingly, the onset of pattern formation at the Turing

instability was preceded by increasing autocorrelation (at lag 1; fig. 6, *C3*). Variance and skewness, however, showed no trend (fig. 6, *C1*, *C2*).

Discussion

Critical transitions are large, self-propelling changes in the state of a system induced by small changes in external conditions (Scheffer et al. 2009). Given that critical transitions occur unexpectedly and may have drastic and irreversible consequences, the ability to estimate their risk is of utmost societal and economic importance. Early warning signals for critical transitions offer such opportunity (Scheffer et al. 2009). If detected early in advance (Biggs et al. 2009), they can help to navigate away from unpleasant surprises.

It has been suggested that the universal phenomenon of critical slowing down close to critical transitions will in practice translate into early warning signals, that is, a rise in correlation and variance (Scheffer et al. 2009). In this study, we show that this is not always true. We found that the shift of arid ecosystems to desert in a scale-dependent feedback model with self-organized regular patterns is not announced by a rise in correlation or variance, despite the fact that critical slowing down does happen. This was the only exception. We found a rise in correlation and variance in space (and less clearly in time) to precede the collapse of vegetation in the two other arid ecosystem models we used. Moreover, we identified similar signatures before the onset of pattern formation that mark the transition of a complete vegetation cover to regular patches of vegetation in the scale-dependent feedback model (table 2).

The failure of correlation and variance to announce the shift to desert in the scale-dependent feedback model suggests that there may be considerable deviations in the behavior of generic indicators in this or similar classes of spatially organized systems when compared with the other two model systems we studied. These deviations appear to be associated with the presence of self-organized regular patterns, which are a consequence of the way feedbacks operate in space for these classes of systems.

In the local positive feedback model, spatial processes are governed by diffusion between neighboring sites (fig. 2, *A1*). Close to transition, random losses of vegetation in each site take longer to be compensated; the vegetation dynamics slow down, and diffusion starts to dominate the patterns. As a result, each site becomes more influenced by biomass dispersed from its neighbors (Dakos et al. 2010). Such strong neighbor effects lead to increasing spatial clustering of vegetation (fig. 2, *A2*). This translates into elevated correlation and variance before a transition.

In the local facilitation model, regeneration of a degraded site depends on the presence of vegetation next to it (fig. 2, *B1*). When aridity increases, colonization of empty sites by vegetation becomes more difficult (slows down), and similar to the local positive feedback model, the regeneration of vegetation in the degraded sites will be influenced more strongly by the presence of vegetated neighbors. As a result, local facilitation becomes the dominant force that leads to clustering around existing irregular patches (fig. 5*A*), again translating into an increase in correlation and variance before transition to desertification.

Things work differently in the scale-dependent feedback model, with its distinct regular vegetation patterns (fig. 2*C*). High regularity of the patterns simply translates into high correlation and variance. As rainfall decreases toward the shift, patterns change in shape, but their regularity remains high, and so do correlation and variance. Only just before the transition, when the regularity of the patterns starts breaking up, do correlation and variance decrease.

Although regular pattern formation appears to mask the performance of variance and correlation as leading indicators in the scale-dependent feedback model, the shape of the patterns themselves reveals much information on the proximity to the upcoming transition (Rietkerk et al. 2004). This may be true for the entire class of ecosystems that exhibit self-organized pattern formation (Rietkerk and van de Koppel 2008), ranging from bogs (Eppinga et al. 2009) to mussel beds (van de Koppel et al. 2005). Similar pattern-based indicators specific to certain classes of systems may be deviations in power laws in systems with scale-invariant patches (Pascual and Guichard 2005), such as the ones produced by the local facilitation model (fig. 5*A*; Kéfi et al. 2007*b*). Although such pattern-based indicators may sometimes be enough to announce specific types of transitions, combining them with correlation and variance may help to reduce the possibility of false alarms. For example, changes in the statistical properties of patch size distributions (such as a decrease in skewness of patch sizes; see fig. A1), together with an increase in skewness of vegetation cover (fig. 4, *B2*), may yield a more robust indicator of an approaching transition than any of those indicators alone. More importantly, pattern-based and generic indicators complement each other. In systems with self-organized regular patterns, changes in the shape of the patterns can be used for announcing desertification (fig. 5*C*), whereas generic indicators (in particular, spatial correlation) can signal the onset of pattern formation: the transition to the appearance of the first degraded sites in the ecosystem (fig. 4, *C3*).

The failure of correlation and variance to signal collapse in systems with self-organized regular patterns suggests that there may be more cases in which these indirect indicators of resilience can fail to signal the risk of upcoming

Table 2: Summary of the performance of leading indicators in the three models used

	Local positive feedback	Local facilitation		Scale-dependent feedback	
Indicator	Up to transition point	Up to percolation point	From percolation to transition point	Up to Turing instability	From Turing instability to transition point
Critical slowing down	+	+	+	+	+
Generic:					
Spatial correlation	+	+	+	+	Fails
Spatial variance	+	+	+	Fails	Fails
Spatial skewness	+	+	+	Fails	+
Temporal correlation	+	+	+	+	Fails
Temporal variance	+	+	+	Fails	Fails
Temporal skewness	Fails	Fails	Fails	Fails	Fails
System specific:					
Patch size distributions	NA[a]	+	+	NA[a]	NA[b]
Pattern shapes	NA[c]	NA[d]	NA[d]	NA[c]	+

Note: NA, not applicable.

[a] No patches.

[b] One-size patches.

[c] No patterns.

[d] Irregular patterns.

transitions. Obviously, we cannot expect such leading indicators to signal the proximity of transitions that are not associated to critical slowing down (Scheffer et al. 2009). However, our results show that even if critical slowing down is present, it may not be reflected by rising correlation or variance. By contrast, the recovery time required for the system to return to equilibrium after a disturbance appears to be a robust indicator of critical slowing down (fig. 3). Indeed, recent work on a similar model system with pattern formation confirms that recovery time upon disturbance increases before desertification (Bailey 2010).

In conclusion, recovery time upon local perturbation experiments may be the most generic and robust indicator of critical slowing down before a transition (van Nes and Scheffer 2007). While elevated correlation and variance may often serve as indirect indicators of critical slowing down, the presence of self-organized regular patterns can suppress change in such indicators. In this particular situation, changes in the patterns themselves are the best indicator of an upcoming transition.

Acknowledgments

We would like to thank I. Hoof for reading and commenting on the article and S. Rinaldi for valuable discussions on bifurcation theory. We also thank two anonymous reviewers for their comments, which greatly helped improve the manuscript. V.D. is supported by a Netherlands Organization for Scientific Research (NWO) grant. S.K.'s research was founded by a fellowship from the Alexander von Humboldt Foundation. The research of M.R. was supported by a personal Vidi grant from the NWO Earth and Life Sciences (NWO-ALW). M.S. is supported by a Spinoza award from the NWO.

APPENDIX

Supplementary Statistics

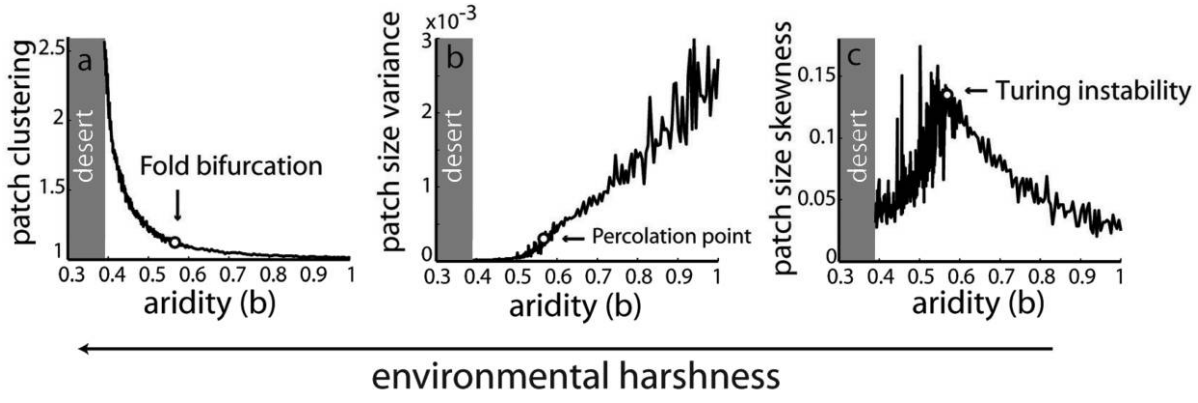

Figure A1: Statistical properties of patch size distributions in the local facilitation model. *a*, Spatial clustering increased (clustering was estimated as $q_{+|+}/\rho_+$, where $q_{+|+}$ is the conditional probability of finding a vegetated cell next to a vegetated cell and ρ_+ is the fraction of vegetated cells in the total grid; van Baalen 2000). *b*, Patch size variance declined up to the transition point. *c*, Patch size skewness exhibited a dual behavior: it rose until the percolation point as the number of large patches decreased and the number of small patches increased. After the percolation point, skewness dropped as the large patches broke down into small ones. The lack of vegetated patches in the local positive feedback model and the regularity of the patches in the scale-dependent feedback model make such estimation not feasible in these two models.

Literature Cited

Aguiar, M. R., and O. E. Sala. 1999. Patch structure, dynamics and implications for the functioning of arid ecosystems. Trends in Ecology & Evolution 14:273–277.

Bailey, R. M. 2010. Spatial and temporal signatures of fragility and threshold proximity in modelled semi-arid vegetation. Proceedings of the Royal Society B: Biological Sciences 278:1064–1071, doi: 10.1098/rspb.2010.1750.

Biggs, R., S. R. Carpenter, and W. A. Brock. 2009. Turning back from the brink: detecting an impending regime shift in time to avert it. Proceedings of the National Academy of Sciences of the USA 106:826–831.

Carpenter, S. R. 2003. Regime shifts in lake ecosystems: pattern and variation. Excellence in Ecology Series. Vol. 15. International Ecology Institute, Oldendorf/Luhe.

Carpenter, S. R., and W. A. Brock. 2006. Rising variance: a leading indicator of ecological transition. Ecology Letters 9:311–318.

Chow, S. N., J. MalletParet, and E. S. VanVleck. 1996. Dynamics of lattice differential equations. International Journal of Bifurcation and Chaos 6:1605–1621.

Dakos, V., E. van Nes, R. Donangelo, H. Fort, and M. Scheffer. 2010. Spatial correlation as leading indicator of catastrophic shifts. Theoretical Ecology 3:163–174.

Donangelo, R., H. Fort, V. Dakos, M., Scheffer, and E. H. van Nes. 2010. Early warnings for catastrophic shifts in ecosystems: comparison between spatial and temporal indicators. International Journal of Bifurcation and Chaos 20:315–321.

Eppinga, M. B., P. C. de Ruiter, M. J. Wassen, and M. Rietkerk. 2009. Nutrients and hydrology indicate the driving mechanisms of peatland surface patterning. American Naturalist 173:803–818.

Guttal, V., and C. Jayaprakash. 2007. Impact of noise on bistable ecological systems. Ecological Modelling 201:420–428.

———. 2008. Changing skewness: an early warning signal of regime shifts in ecosystems. Ecology Letters 11:450–460.

———. 2009. Spatial variance and spatial skewness: leading indicators of regime shifts in spatial ecological systems. Theoretical Ecology 2:3–12.

Hastings, A., and D. B. Wysham. 2010. Regime shifts in ecological systems can occur with no warning. Ecology Letters 13:464–472.

Held, H., and T. Kleinen. 2004. Detection of climate system bifurcations by degenerate fingerprinting. Geophysical Research Letters 31:L23207.

HilleRisLambers, R., M. Rietkerk, F. van den Bosch, H. T. Prins, and H. De Kroon. 2001. Vegetation pattern formation in semi-arid grazing systems. Ecology 82:50–61.

Holling, C. S. 1973. Resilience and stability of ecological systems. Annual Review of Ecology and Systematics 4:1–23.

Ives, A. R., B. Dennis, K. L. Cottingham, and S. R. Carpenter. 2003. Estimating community stability and ecological interactions from time-series data. Ecological Monographs 73:301–330.

Janssen, R. H. H., M. B. J. Meinders, E. H. van Nes, and M. Scheffer. 2008. Microscale vegetation-soil feedback boosts hysteresis in a regional vegetation-climate system. Global Change Biology 14: 1104–1112.

Judd, S. L., and M. Silber. 2000. Simple and superlattice Turing patterns in reaction-diffusion systems: bifurcation, bistability, and parameter collapse. Physica D 136:45–65.

Kéfi, S., M. Rietkerk, M. van Baalen, and M. Loreau. 2007*a*. Local

facilitation, bistability and transitions in arid ecosystems. Theoretical Population Biology 71:367–379.

Kéfi, S., M. Rietkerk, C. L. Alados, Y. Pueyo, V. P. Papanastasis, A. ElAich, and P. C. de Ruiter. 2007*b*. Spatial vegetation patterns and imminent desertification in Mediterranean arid ecosystems. Nature 449:213–217.

Kéfi, S., M. Rietkerk, M. Roy, A. Franc, P. C. de Ruiter, and M. Pascual. 2011. Robust scaling in ecosystems and the meltdown of patch size distributions before extinction. Ecology Letters 14:29–35.

Keitt, T. H., M. A. Lewis, and R. D. Holt. 2001. Allee effects, invasion pinning, and species' borders. American Naturalist 157:203–216.

Knowlton, N. 1992. Thresholds and multiple stable states in coral reef community dynamics. American Zoologist 32:674–682.

Legendre, P., and M. J. Fortin. 1989. Spatial pattern and ecological analysis. Plant Ecology 80:107–138.

Millennium Assessment. 2005. Ecosystems and human well-being: our human planet: summary for decision makers. Island, Washington, DC.

Neumaier, A., and T. Schneider. 2001. Estimation of parameters and eigenmodes of multivariate autoregressive models. ACM Transactions on Mathematical Software 27:27–57.

Pascual, M., and F. Guichard. 2005. Criticality and disturbance in spatial ecological systems. Trends in Ecology & Evolution 20:88–95.

Reynolds, J. F., D. M. S. Smith, E. F. Lambin, B. L. Turner, M. Mortimore, S. P. J. Batterbury, T. E. Downing, et al. 2007. Global desertification: building a science for dryland development. Science 316:847–851.

Rietkerk, M., and J. van de Koppel. 2008. Regular pattern formation in real ecosystems. Trends in Ecology & Evolution 23:169–175.

Rietkerk, M., M. C. Boerlijst, F. van Langevelde, R. HilleRisLambers, J. van de Koppel, L. Kumar, H. H. T. Prins, and A. M. de Roos. 2002. Self-organization of vegetation in arid ecosystems. American Naturalist 160:524–530.

Rietkerk, M., S. C. Dekker, P. C. de Ruiter, and J. van de Koppel. 2004. Self-organized patchiness and catastrophic shifts in ecosystems. Science 305:1926–1929.

Scheffer, M. 1998. Ecology of shallow lakes. Chapman & Hall, London.

Scheffer, M., S. Carpenter, J. A. Foley, C. Folke, and B. Walker. 2001. Catastrophic shifts in ecosystems. Nature 413:591–596.

Scheffer, M., J. Bascompte, W. A. Brock, V. Brovkin, S. R. Carpenter, V. Dakos, H. Held, E. H. van Nes, M. Rietkerk, and G. Sugihara. 2009. Early-warning signals for critical transitions. Nature 461:53–59.

Shnerb, N. M., P. Sarah, H. Lavee, and S. Solomon. 2003. Reactive glass and vegetation patterns. Physical Review Letters 90:038101.

Strogatz, S. H. 1994. Nonlinear dynamics and chaos with applications to physics, biology, chemistry and engineering. Perseus, Cambridge.

Turing, A. M. 1952. The chemical basis of morphogenesis. Philosophical Transactions of the Royal Society B: Biological Sciences 237:37–72.

van Baalen, M. 2000. Pair approximation for different spatial geometries. Pages 359–387 *in* U. Diekmann, R. Law, and J. A. J. T. Metz, eds. The geometry of ecological interactions: simplifying spatial complexity. Cambridge University Press, Cambridge.

van de Koppel, J., M. Rietkerk, N. Dankers, and P. M. Herman. 2005. Scale-dependent feedback and regular spatial patterns in young mussel beds. American Naturalist 165:E66–E77.

van Nes, E. H., and M. Scheffer. 2003. Alternative attractors may boost uncertainty and sensitivity in ecological models. Ecological Modeling 159:117–124.

———. 2005. Implications of spatial heterogeneity for regime shifts in ecosystems. Ecology 86:1797–1807.

———. 2007. Slow recovery from perturbations as a generic indicator of a nearby catastrophic shift. American Naturalist 169:738–747.

von Hardenberg, J., E. Meron, M. Shachak, and Y. Zarmi. 2001. Diversity of vegetation patterns and desertification. Physical Review Letters 8719:198101.

Wissel, C. 1984. A universal law of the characteristic return time near thresholds. Oecologia (Berlin) 65:101–107.

Associate Editor: Mathew A. Leibold
Editor: Judith L. Bronstein